

1 **Supporting Information**

2

3 **Unveiling Critical Role of Metal Oxide Infiltration in Controlling the Surface Oxygen**

4 **Exchange Activity and Polarization of SrTi<sub>1-x</sub>Fe<sub>x</sub>O<sub>3-δ</sub> Perovskite Oxide Electrodes**

5

6 Hyunseung Kim<sup>+,a</sup>, Han Gil Seo<sup>+,b,c</sup>, Sejong Ahn<sup>a</sup>, Harry L. Tuller<sup>\*,b</sup>, and WooChul Jung<sup>\*,d</sup>

7

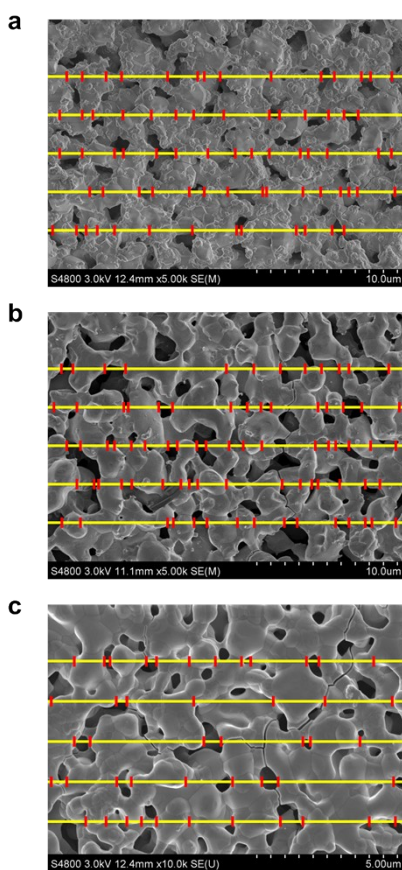
8 <sup>a</sup> Department of Materials Science and Engineering, Korea Advanced Institute of Science and Technology  
9 (KAIST), Daejeon 34141, Republic of Korea

10 <sup>b</sup> Department of Materials Science and Engineering, Massachusetts Institute of Technology (MIT), Cambridge,  
11 MA 02139, USA

12 <sup>c</sup> Department of Materials Science and Engineering, Dankook University, Cheonan, 31116 Republic of Korea

13 <sup>d</sup> Department of Materials Science and Engineering, Seoul National University, Seoul 08826, Republic of Korea

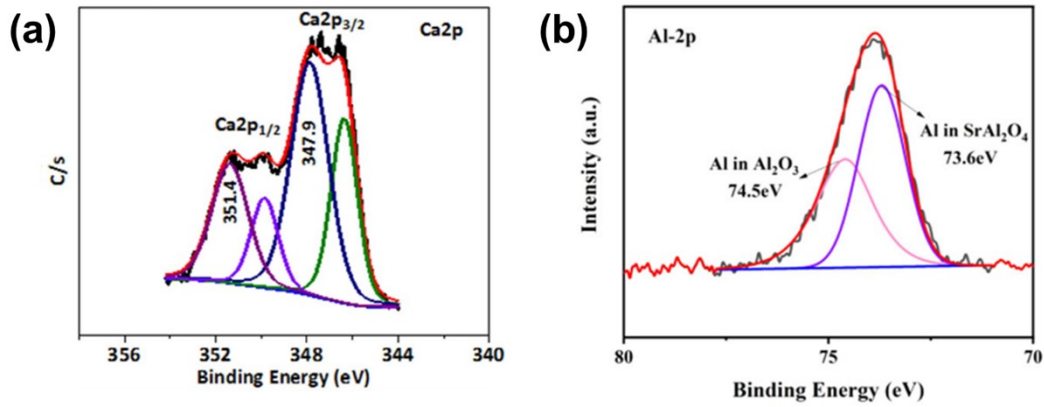
14 **+ These authors contributed equally to this work.**



15

16 **Figure S1. Scanning electron microscopy images of specimens used in determining**  
17 **surface-area-to-volume ratios. (a)  $\text{SrTi}_{0.65}\text{Fe}_{0.35}\text{O}_{3-\delta}$ , (b)  $\text{SrTi}_{0.5}\text{Fe}_{0.5}\text{O}_{3-\delta}$ , and (c)**  
18  **$\text{SrTi}_{0.2}\text{Fe}_{0.8}\text{O}_{3-\delta}$ .**

19



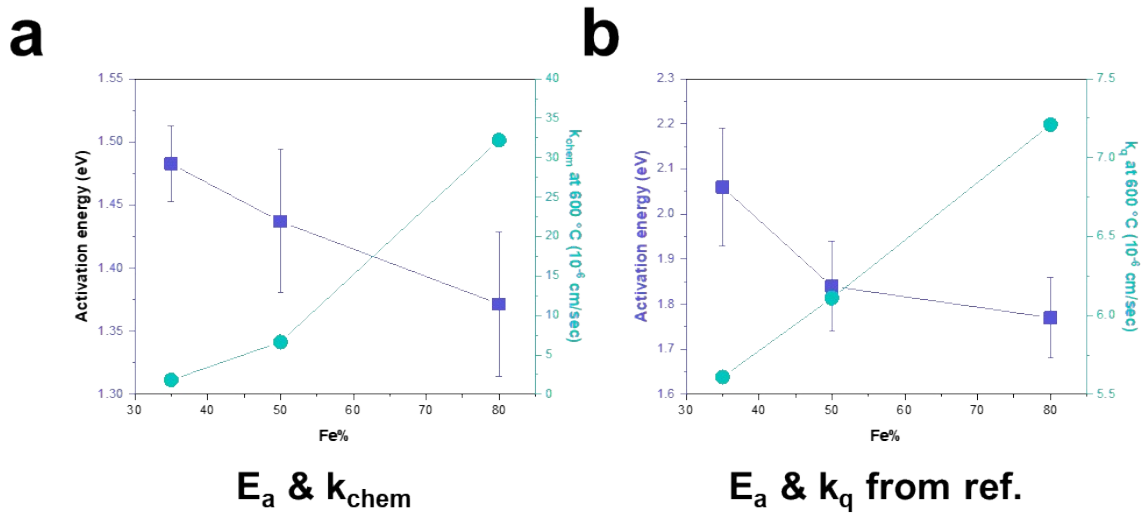
Figure

21

22 **S2. X-ray photoelectron spectroscopy (XPS) analysis on (a) Ca 2p of CaTiO<sub>3</sub>, showing a**  
 23 **Ca 2p<sub>3/2</sub> peak at 347.9 eV, compared with CaCO<sub>3</sub>, which exhibits a Ca 2p<sub>3/2</sub> peak at 346**  
 24 **eV;<sup>[1]</sup> and (b) Al 2p of Al<sub>2</sub>O<sub>3</sub>, displaying a peak at 74.5 eV, compared with SrAl<sub>2</sub>O<sub>4</sub>, which**  
 25 **shows a peak at 73.6 eV.<sup>[2]</sup>**

26

27



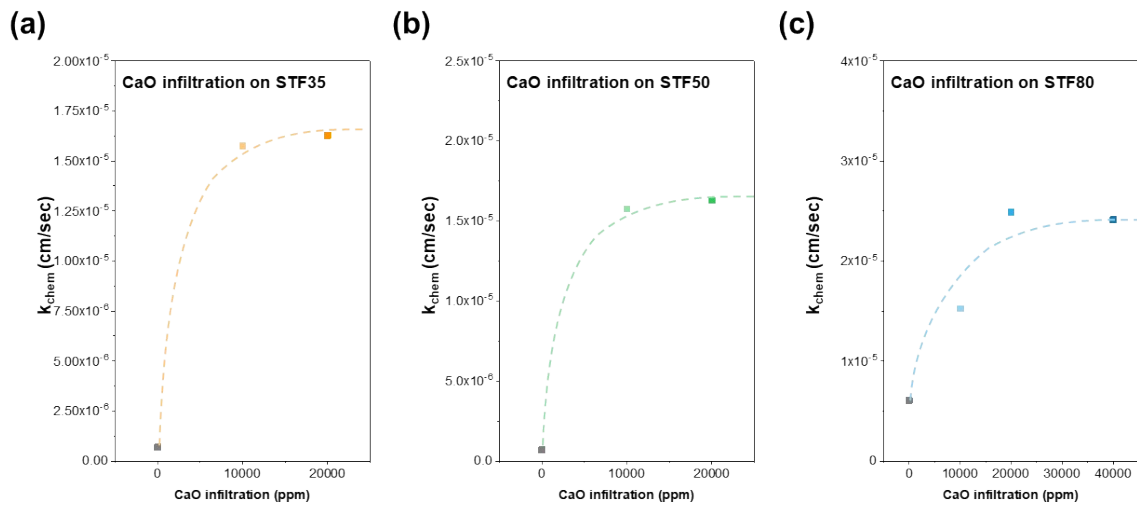
29

30 **Figure S3. Activation energy (in violet, left) and  $k_{chem}$  at 600 °C (in turquoise, right) as**  
 31 **function of iron content in SrTi<sub>1-x/100</sub>Fe<sub>x/100</sub>O<sub>3-δ</sub> (STFx). (b) Activation energy (in violet,**  
 32 **left) and  $k_q$  at 600 °C (in turquoise, right) of STFx, derived from electrochemical**  
 33 **impedance spectroscopy measurements on thin-film. Source: Jung et al.<sup>[3]</sup>**

34

35

36

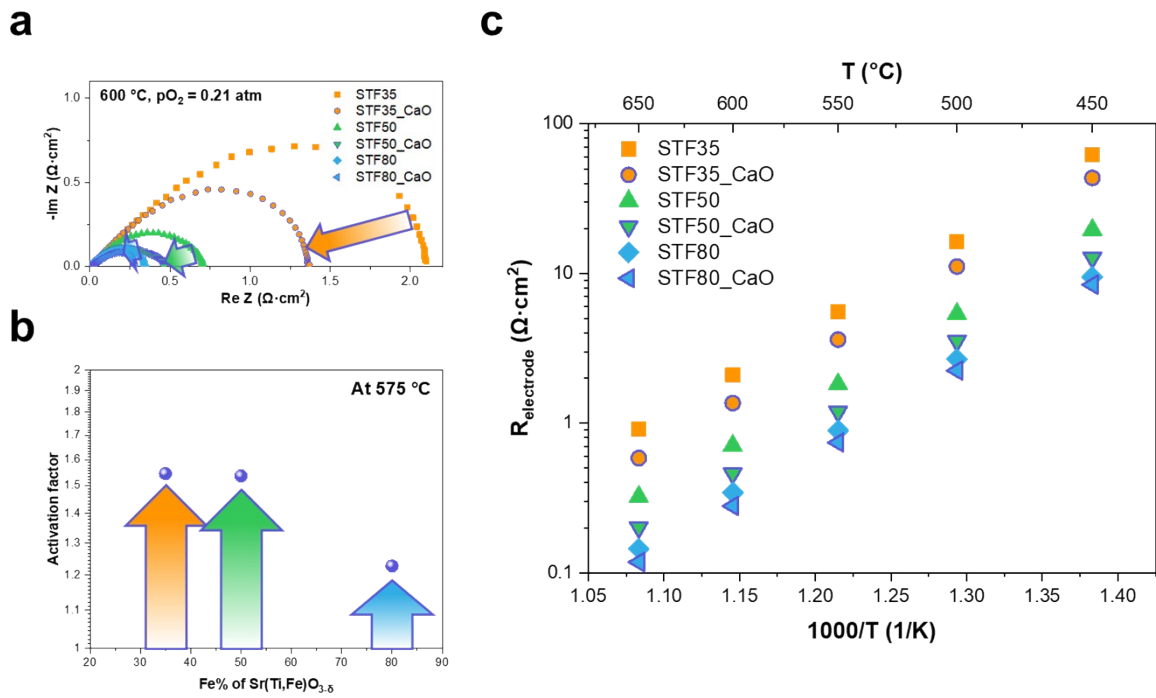


37

38 **Figure S4. Surface oxygen exchange coefficient,  $k_{chem}$ , of (a)  $SrTi_{0.65}Fe_{0.35}O_{3-\delta}$ , (b)**  
39  **$SrTi_{0.5}Fe_{0.5}O_{3-\delta}$ , and (c)  $SrTi_{0.2}Fe_{0.8}O_{3-\delta}$  at 525 °C as a function of CaO infiltration amount.**

40

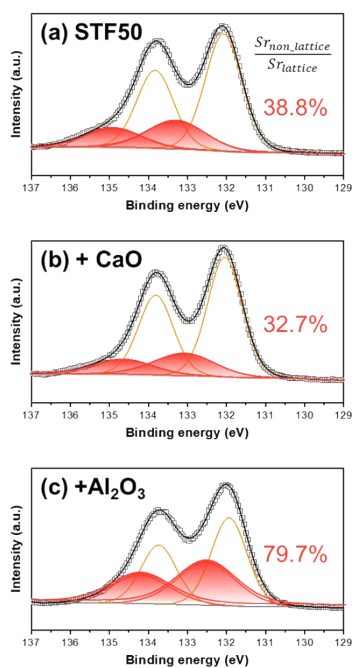
41



42

43 **Figure S5. Enhanced surface activity of SrTi<sub>0.65</sub>Fe<sub>0.35</sub>O<sub>3-δ</sub>, SrTi<sub>0.5</sub>Fe<sub>0.5</sub>O<sub>3-δ</sub>, and**  
 44 **SrTi<sub>0.2</sub>Fe<sub>0.8</sub>O<sub>3-δ</sub> by CaO infiltration. (a) Electrochemical impedance spectroscopy Nyquist**  
 45 **plot measured at 600 °C for symmetrical cells (Electrode|(Sm,Ce)O<sub>2-δ</sub>|Electrode). (b)**  
 46 **Activation factor calculated for each SrTi<sub>1-x/100</sub>Fe<sub>x/100</sub>O<sub>3-δ</sub> (STFx) cell measured at 575 °C.**  
 47 **(c) Arrhenius plots of STFx electrode resistance ( $R^{electrode}$ ) before and after CaO**  
 48 **infiltration.**

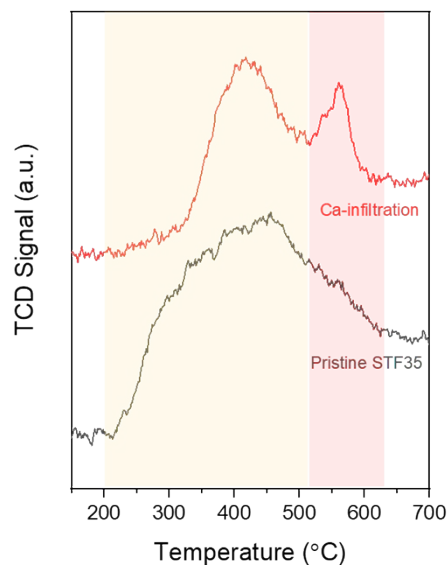
49



50

51 **Figure S6. X-ray photoelectron spectroscopy (XPS) analysis on Sr 2p for (a)**  
 52 **SrTi<sub>0.5</sub>Fe<sub>0.5</sub>O<sub>3-δ</sub> (STF50), (b) CaO-infiltrated STF50, and (c) Al<sub>2</sub>O<sub>3</sub>-infiltrated STF50 after**  
 53 **annealing at 700 °C for 10 hours.**

54



55

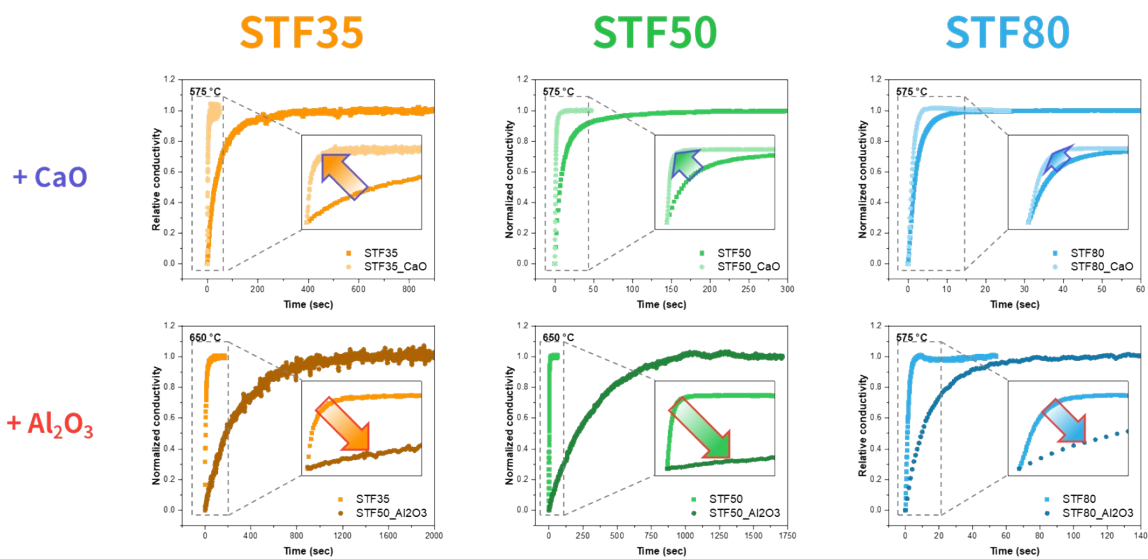
56 **Figure S7. CO<sub>2</sub> temperature programmed desorption (CO<sub>2</sub>-TPD) analysis result on the**  
 57 **pristine and CaO-infiltrated STF35.**

58

59 To further confirm that the CaO was uniformly deposited across the entire surface, CO<sub>2</sub>  
 60 temperature programmed desorption analysis was conducted on both the pristine and CaO-  
 61 infiltrated STF35. Here, two distinct regions of CO<sub>2</sub> desorption were observed: desorption of  
 62 weakly adsorbed CO<sub>2</sub> at lower temperatures (200-500 °C) and strongly adsorbed CO<sub>2</sub> at high  
 63 temperatures (500-600 °C). The CaO-infiltrated specimen, which strongly chemisorbed CO<sub>2</sub>,  
 64 exhibited an additional peak at 560 °C compared to the pristine sample, indicating the presence  
 65 of additional strong base sites, which is in good agreement with our observations. It also shows  
 66 that CaO infiltration not only caused the appearance of a high-temperature peak for strongly  
 67 adsorbed CO<sub>2</sub> in the 500-600 °C range but also shifted the peak for weakly adsorbed CO<sub>2</sub> in  
 68 the 200-500 °C range toward higher temperatures. This indicates that the CaO infiltration  
 69 enhanced the overall CO<sub>2</sub> adsorption strength of the STF surface, suggesting the infiltration  
 70 was applied across the entire surface.

71





72

73 **Figure S8. Conductivity relaxation profiles measured on SrTi<sub>0.65</sub>Fe<sub>0.35</sub>O<sub>3-δ</sub>,**  
 74 **SrTi<sub>0.5</sub>Fe<sub>0.5</sub>O<sub>3-δ</sub>, and SrTi<sub>0.2</sub>Fe<sub>0.8</sub>O<sub>3-δ</sub> samples before and after infiltration of CaO and**  
 75 **Al<sub>2</sub>O<sub>3</sub>.**

76

77

78

79 **References:**

- 80 [1] M. A. Ehsan, R. Naeem, V. McKee, A. Rehman, A. S. Hakeem, M. Mazhar, *Journal of*  
81 *Materials Science: Materials in Electronics* **2019**, *30*, 1411.
- 82 [2] B. Lu, M. Shi, Z. Pang, Y. Zhu, Y. Li, *Journal of Materials Science: Materials in*  
83 *Electronics* **2021**, *32*, 17382.
- 84 [3] W. Jung, H. L. Tuller, *Adv Energy Mater* **2011**, *1*, 1184.

85